PIV methodology for small scale measurement

Miloš Kašpárek[1,*], *Ludmila* Nováková[2], and *Josef* Adamec[1]

[1]CTU in Prague, Department of fluid dynamics and thermodynamics, 16607 Prague 6, Czech Republic
[2]J.E. Purkyně University in Usti na Labem, Department of Energy and Electrical Engineering, 40096 Usti nad Labem, Czech Republic

Abstract. Measurement of velocity fields by PIV method is often limited by the scale of the measured model. This is doubly true for the stereo PIV method. Problems of measurement in small (but still macroscopic) scales are associated with optical distortions in the optical path of the camera. Additionally, there is a calibration problem for stereo PIV. Therefore, this paper is devoted to the description of PIV methodology for measurement in small geometrical scales. The idealized transparent model of hemodialysis vascular access was used in this paper. This model had realistic vascular access dimensions (6 mm in diameter). A special working blood-mimicking fluid (BMF) was mixed with a refractive index matching that of the model. The refraction and distortion of light passing through the interface between the model and the fluid was so small, that it was possible to calibrate the stereo PIV outside the measured model. The accuracy of this calibration is discussed and verified by measuring the velocity field on a straight section of the vascular access model for laminar flow.

1 Introduction

Method Particle Image Velocimetry (PIV) and its modifications are often used in fluid mechanics to measure velocity fields. The successful use of this measuring method is conditioned by a large number of assumptions. The sources of PIV measurement uncertainty are generally connected either with the method of data analysis or with the experimental setup. The former uncertainty sources are discussed in [12],[2],[9] the latter are, for example, the correct selection of marking particles to be added to the fluid, sufficient and uniform illumination of the measurement surface, or quality optical access to the entire measurement area. The necessity to ensure good optical access to the measurement area limits the model dimensions in which the PIV method can be used successfully. With the small dimensions of the model, it is difficult to ensure good optical access because the small dimensions of the model are associated with areas of large optical deformation. These optical deformations result in significant errors in the measurement. In the case of a modification of the PIV method, where all three components of the velocity (stereo PIV) are monitored in the measured area, it is necessary to perform calibration before the measurement itself. Calibration in the small size model is very difficult, even impossible.

Optical distortions are due to the curvature of the measured model in which the measurement is performed. Of course, the greater curvature of the model in the measured area also leads to greater optical deformations that occur at the interface of the two materials. Reflections are another optical defect associated with light reflection at the interface of two materials. These reflections introduce the signal deterioration into the measurement.

When using the stereo PIV method for the measurement, the measured area is monitored by the two cameras. These cameras track the measurement area at an angle, which allows measuring, in addition to the two velocity components, the third velocity component that is perpendicular to the measured area. Therefore, in order to evaluate all velocity components from the captured images of the measured area, the calibration is required [11], [10]. The transformation matrix can be calculated from the recording of the target image in several predefined positions in the measured model. There are several ways of calibration. The most commonly used calibration is the use of a calibration target, which is located in the measured area. For example, the calibration target consists of an array of circular dots with the precisely defined dimensions. By recording the image of the calibration target at several predefined positions in the measured model, it is then possible to calculate the transformation matrix. For small-scale stereo PIV measurements, calibration has several problems: an optical distortion problem distorting the calibration target, realizing the movement of the target in the model, and creating the calibration target itself.

Despite these difficulties, it is possible to measure velocity fields by the stereo PIV in the small size models. First of all, it is necessary to remove optical deformations from the model / fluid interface. The removal of the optical defects is dealt with in several works [15], [4], [7], [1], namely by the change of the refractive index of used fluid. Specifically, this means that the refractive index value of the fluid is changed so that the refractive index of the light of the fluid is identical (very similar) to that of

* Corresponding author: milos.kasparek@fs.cvut.cz

the refractive index of light of the model. The smaller the difference between the refractive indices of the light, the smaller the optical deformation. The refractive index of light of the fluid can be changed by adding an additive to the fluid that is soluble in the fluid. The choice of additive that changes the refractive index of light is also associated with the requirements for the properties of the resulting working fluid. The elements used for changing the refractive index of light are, for example, sodium iodide [1], [8], zinc iodide [4], potassium thiocyanate [3] or glycerine [15]. The refractive index of the light of the material from which the measured model is made must also be taken into account. The material of the model should be chosen so that it has a refractive index similar to that of untreated fluid [5]. Generally speaking, it should have the lowest possible refractive index of light. Such material is, for example, Sylgard 184. If accordance of the refractive indexes of light are very good, it is possible to make the calibration outside the measured model and then use the obtained transformation matrices for measurement in the model [14].

This thesis deals with the accurate description of the calibration for the stereo PIV measurement in the small size model and its evaluation. The vascular access model is used for the measurement, which is used as well in hemodialysis, maintaining the realistic dimensions of the vein and the dialysis needles. The diameter representing the diameter of the vein is 6 mm. Measurement of the velocity field for the comparison with the theory and thus confirmation of the success of the calibration is performed on the straight part of the model, where the flow is not influenced by the inserted needles.

The vascular access model was made using the casting technology, where the template representing the internal geometry was made with the water-soluble material. The template was made by using 3D printing and its surface was modified to be hydraulically smooth.

2 Removal of the optical defects

Changing the refractive index of the light of a fluid is difficult for several reasons. Substances added to the fluid can fundamentally alter its rheological properties, often being chemically hazardous to the environment or they are expensive. Therefore, it is advisable to select the material of the model so that the refractive index of the light is as close as possible to the base component of the working fluid solution. The distilled water is the most often used liquid as the base component of the working fluid. The refractive index of the light of the distilled water is 1.33 (1). In this work, the measured model was made by silicone elastomer with the trade name Sylgard 184. This material was chosen due to its low refractive index of the light compared to the other commonly used materials for the model making. The refractive index of the light of this silicone elastomer is 1,414 (1) [15]. The working fluid was mixed from the distilled water, glycerine and sodium iodide. The weight ratio of these components was 47.38% distilled water, 36.94% glycerine and 15.68% sodium iodide [15]. The resulting refractive index of the light of the working fluid was 1.413 (1). In Figure 1 there is a comparison of the optical deformation in the model with the water-glycerine solution (refractive index of light 1.387 (1)) and the optical deformation in the model with the working fluid. The model with the given solutions was placed on a black and white checkerboard. This makes it possible to assess the optical deformation. Although the refractive index of the water-glycerine solution is close to the refractive index of the material of the model, optical distortion is still visible in the image. The second solution (working fluid) shows that there is no visible optical deformation of the measured area. The refractive index of the working fluid and the model material was practically identical.

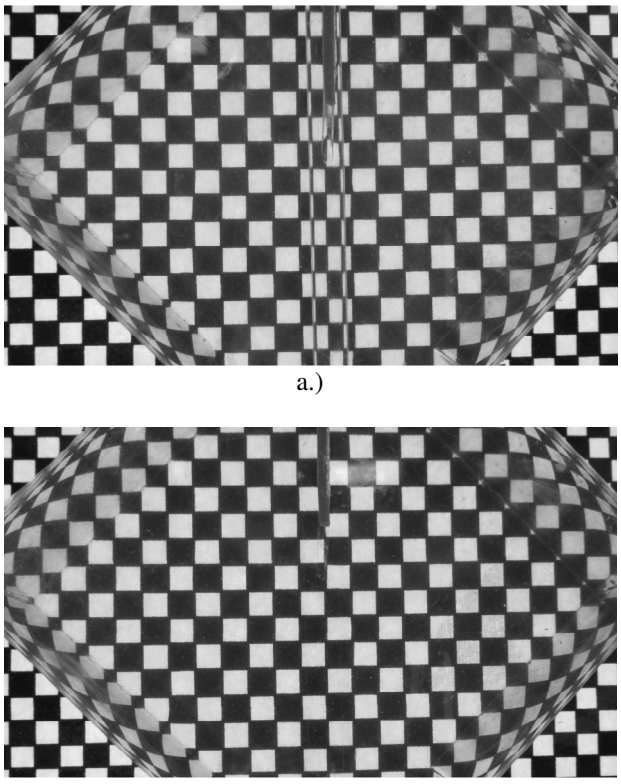

a.)

b.)

Fig. 1. Optical deformation of the measured area. a.) the model with the solution of distilled water and glycerine. b.) the model with the solution of distilled water, glycerine and sodium iodide.

3 Calibration

When the refractive index of the measured model and the working fluid is identical (very similar), the optical distortions are removed. This makes it possible to calibrate the stereo PIV as if it was an external flow. This means that the model is replaced by the calibration target.

In this work the calibration target consisting of the circular dots was used (Fig. 2). The central dot had a diameter of 0.6 mm, the four dots determining the direction of the „x" axis and the „y" axis had a diameter of 0.3 mm, and the remaining dots had a diameter of 0.45 mm. The spacing between the dots is 0.75 mm. The total number of dots on the calibration target was 225 dots. The calibration target was placed in a equipment that delimited

the location of the target in the „y" direction. The equipment was placed on the two feets. The first feet allowed movement of the calibration target in the „x" direction. The second feet allowed movement of the calibration target in the „z" direction. The calibration target placed in the equipment was positioned by the displacements to the starting position. The starting position was in the measured plane and the calibration target was positioned so that the central dot was in the tube axis of the measured model. The pair of calibration target images were created in this position. The target was then shifted twice 0.5 mm in the direction of „z" axis in the positive and negative directions from the starting position. The pair of calibration target images were obtained at each new position. The transformation matrices for both cameras were evaluated from the obtained images of the calibration target at all positions by using the Dantec Dynamic studio software. After calculating the transformation matrices, a self-calibration was performed to improve the transformation matrices. The self-calibration has partially suppressed errors that could have been caused by improper placement of the calibration target in the equipment (eg small rotation of the calibration target).

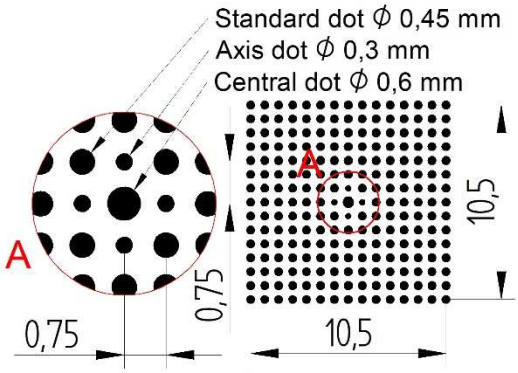

Fig. 2. Calibration target.

4 Setup of the experiment

Scheme of the experiment for the verification measurements is shown in Figure 3. The measured area of the model is illuminated by a laser sheet. The cameras capture the measured area at an angle. The angle between the cameras was 90 °. The Scheimpflug condition was met. The volumetric flow rate was adjusted using a flowmeter and a valve downstream of the flowmeter. The measured model was made of Sylgard 184, which has a refractive index of 1,414 (1). The working fluid was a mixture of the distilled water, glycerine and sodium iodide [15]. The refractive index of the light of the working fluid was 1.413 (1) and the dynamic viscosity was 4.31 mPa.s [15]. The measurement confirming the feasibility of the calibration outside the measured model was performed on a straight section of the vascular access model. The measured mode was characterized by Reynolds number Re = 1000.

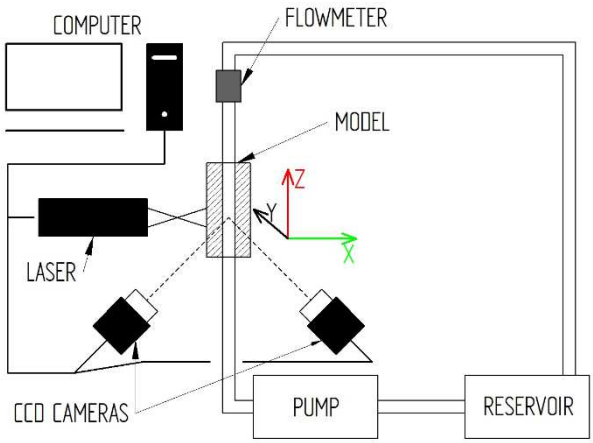

Fig. 3. Scheme of experiment.

5 Results

Figure 4 shows images of the calibration target from both cameras and their transformed images. The transformation matrices obtained by the calibration were used to transform the image. These images can be used as a first indicator of whether the calibration itself has been performed correctly. It is clear from the recorded images of the target that the spatial deformation occurs due to the angle at which the cameras capture the area with the calibration target. Transforming these images leads to the elimination of the spatial deformation and the calibration target takes the shape and the dimensions, like when viewed perpendicularly to the calibration target. The transformed image of the calibration target indicates that the computed transformation matrices work. The success of the image transformation (or transformation matrices obtained from calibration) was determined by the difference of distances („Δx") between individual dots in the x-axis direction and the difference of distances („Δy") between individual dots in the x-axis direction „ y"

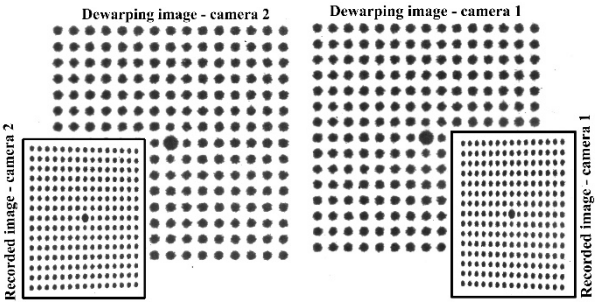

Fig. 4. Transformed images from camera 1 and camera 2.

Figure 5 shows the deviation of the distance „Δx" from the transformed image of the calibration target from the actual distance „Δx". The deviation is on the vertical axis of the graph and it is given in percentage. The horizontal axis shows the columns between which the deviation is calculated. Individual deviations then correspond to the rows of the calibration target. The graph shows that the shape of deviation that oscillates around zero is the same for all rows of the calibration target. The dots in the outer rows of the calibration target show that

the deviation is increasing (green dashed line), reaching up to 6%. This is due both, the print quality of the calibration target and the fact that the endpoints of the calibration target have not been sufficiently focused. For other dots of the calibration target, the deviation is within ± 2%. The red dashed lines then show the progress and the deviation values at the point where the calibration target dots are located directly or in close proximity to the measured area. Here you can see that the deviation is below 2%. Which is a very good conformity. Figure 6 shows the deviation of the distance „Δy" from the transformed image of the calibration target from the actual

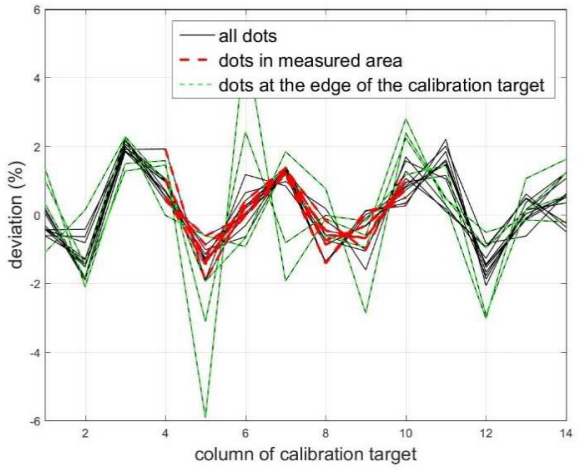

Fig. 5. Deviation of the distance between the dots of the transformed calibration target („Δx") in the „x" axis direction.

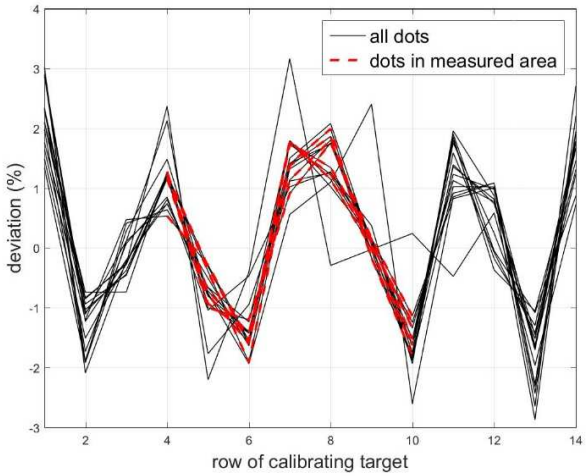

Fig. 6. Deviation of the distance between the dots of the transformed calibration target („Δy") in the „y" axis direction.

distance „y". The deviation is on the vertical axis of the graph and it is given in percentage. The horizontal axis shows the columns between which the deviation is calculated. The individual deviations then correspond to the columns where the deviation was evaluated. The graph shows that the deviation was within ± 3%. The red dashed lines then show the progress and the deviation values at the point where the calibration target dots are located directly or in the close proximity to the measured area. For these dots, the deviation is within ± 2%. The accuracy of the image transformation achieved by the calibration matrices obtained from calibration is very good due to the dimensions of the calibration target and dimensions of the measured area.

The velocity field was evaluated from the data obtained from the experiment by the transformation matrices. Two velocity profiles „w" were obtained from the velocity field. „w" is a velocity in z-direction. The first velocity profile was obtained by horizontal sectioning of the measured area. The second velocity profile was obtained by the vertical sectioning of the measured area. Figure 7a shows a comparison of the vertical section velocity profile with the theoretical laminar flow velocity profile. Figure 7b shows a comparison of the horizontal velocity profile with the theoretical laminar flow velocity profile. For both velocity profile comparisons, it can be seen that it copies the theoretical speed profile with a very

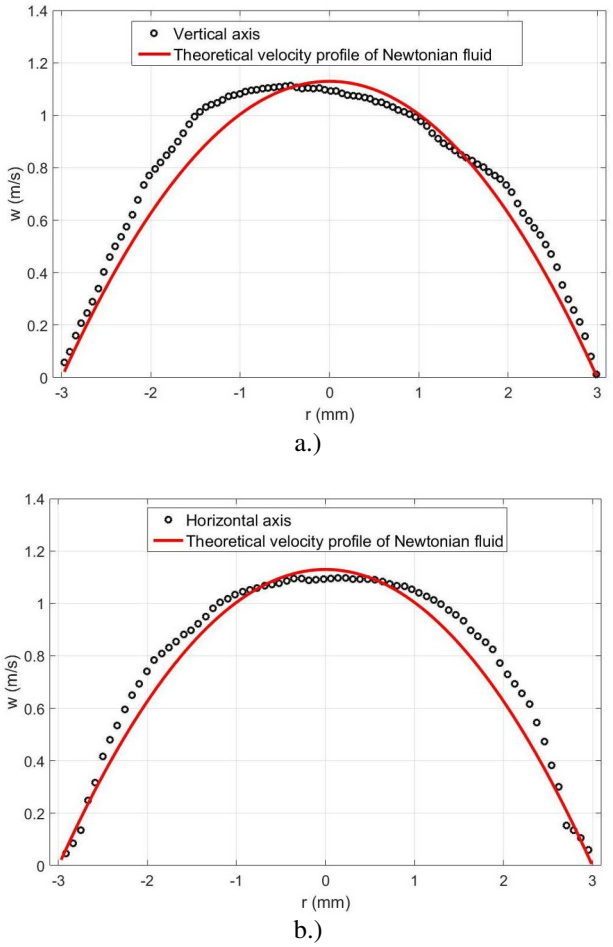

Fig. 7. Comparison of the experimentally measured velocity profile „w" with the laminar theoretical velocity profile. a.) Comparison in the vertical section through the measured area. b.) Comparison in the horizontal section through the measured area.

good accuracy. However, there is a slight asymmetry in both velocity profiles. The laminar velocity profile is extremely sensitive to small disturbances due to the heat convection or the minor misalignments of the tube segments or the minor irregularities of the tube surface. These disturbances lead to speed profile asymmetry [13].

Further the normal velocities of the profiles „u" and „v" were compared. „u" is velocity in „y" axis direction and „v" velocity in „x" axis direction. These profiles were

created in the vertical section through the measured area. The comparison is made by using the percentage ratio between the „u" and „v" velocity profile and the profile of „w" velocity. As a result, there is obtained the percentage deviation that results from the measurement. This ratio is created for both „u" and „v" velocities. From the graph in Figure 8, it can be seen that for both velocities the measurement deviation was constant and the deviation increased in the walls vicinity. For the normal velocity, „u", the average deviation was 1.8%. For the normal velocity, „v", the average deviation was then 4.3%. These deviations in the measurement are associated with the calibration target, where even a slight deviation of the calibration target from the measured plane results in a deviation in the measurement [13], [6].

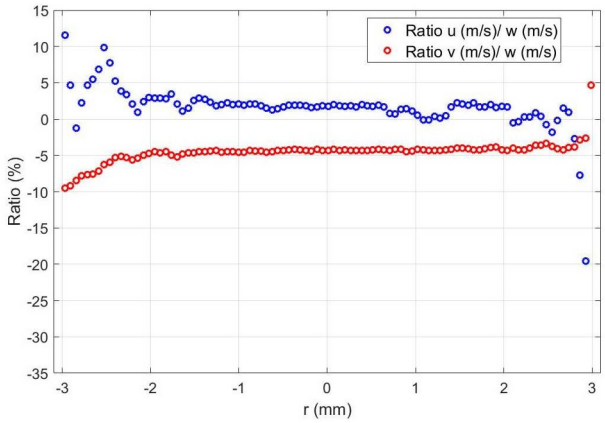

Fig. 8. Comparison of the normal velocities „U" and „V".

6 Discusion

Using the stereo PIV calibration outside the measured model, it is possible to obtain the transformation matrices that can be applied to the measured data and obtain velocity fields in the models with very small dimensions in order of millimetres. The model used in this work had a diameter of 6 mm in the measured area. This fact was confirmed by the comparison of velocity profiles obtained using these transformation matrices with the theoretical laminar velocity profile. The main prerequisite for the success of this method is in a good comparison of the refractive index of the light of the model material and the working fluid. Calibration accuracy is largely linked to the quality of the calibration target. The quality of the calibration target is more difficult to ensure due to the size of the calibration target dots. The dots must be of the size of the sufficient numbers of dots in the measured area. This method of the calibration also enables the measurement of velocity fields using the stereo PIV method in the models with very complex geometry, where there is not possible to place the calibration target in the measured area.

References

1. Bai, K., Katz, J.: On the refractive index of sodium iodide solutions for index matching in PIV, Exp Fluids, 55:1704, 2014
2. Fei, R. & Merzkirch, W.: Exp Fluids (2004) 37: 559. https://doi.org/10.1007/s00348-004-0843-x
3. Gijsen, F.J., van de Vosse, F.N., Janssen, J.D.: The influence of the non-Newtonian properties of blood on the flow in large arteries: steady flow in a carotid bifurcation model. J Biomech 32:601, 1999
4. Hassa, Y.A, Dominquez-Ontiveros, E.E.: Flow visualization in a pebble bed reactor experiment using PIV and refractive index matching techniques, Nuclear Engineering and Design 238, 3080-3085, 2008
5. Jermy M.: Making it clear: Flexible, transparent laboratory flow models for soft and hard problems, Conference on Experimental Heat Transfer, Fluid Dynamics and Thermodynamics, 2013 Lisabon, Portugal, 2013, Conference Contribution
6. Lawson, N.J., Wu, J.: Three-dimensional particle image velocimetry: error analysis of stereoscopic techniques, Meas. Sci. Technol., 8, 894-900, 1997
7. McEvoy, J., Persoons, T.: Aqueous Ammonium Thiosulfate as a working fluid for refractive index matched PIV applications, 9th World Conference on Experimental Heat Transfer, Fluid Mechanics and Thermodynamics ; 2017
8. Narrow, T.L., Yoda, M., Abdel-Khalik, S.I.: A simple model for the refractive index of sodium iodide aqueous solutions, Experiments in Fluids 28, 282-283, 2000
9. Novotny J., Novakova L. and Machovska I.: Advanced metric for particle image velocimetry accuracy estimation 19th Int. Symp. on Applications of Laser and Imaging Techniques to Fluid Mechanics, Lisbon, Portugal, 2018
10. Prasad, A.K.: Stereoscopic particle image velocimetry, Experiments in fluids, Experiments in Fluids, volume 29, 103-116, 2000
11. Raffel M., Willert C. E., Wereley S. T., Kompenhans J. : Particle Image Velocimetry A Practical Guide Second Edition, ISBN 978-3-540-72307-3 Second Edition Springer Berlin Heidelberg New York, 2007
12. Raffel M., Willert C.E., Scarano F., Kähler C.J., Wereley S.T., Kompenhans J.: PIV Uncertainty and Measurement Accuracy. In: Particle Image Velocimetry. Springer, Cham, 2018
13. van Doorne, C.W.H., Westerweel, J.: Measurement of laminar, transitional and turbulent pipe flow using Stereoscopic-PIV, Experimental Fluids, 42,259-279,2007
14. Yagi, T., Sato A., et al.: Experimental insights into flow impingement in cerebral aneurysm by stereoscopic particle image velocimetry: transition from a laminar régime, J. of the Royal Society Interface, 10, 2013
15. Yousif, M.Y., Holdsworth, D.W., Poepping T.L. : A blood-mimicking fluid for particle image velocimetry with silicone vascular models, Exp Fluids 50:769–774, 2011